PHILOSOPHICAL TRANSACTIONS OF THE ROYAL SOCIETY A MATHEMATICAL, PHYSICAL & ENGINEERING SCIENCES

Infrared absorption spectroscopy of D_3: an investigation into the formation mechanisms of triatomic hydrogenic species

T. Amano and Man Chor Chan

Phil. Trans. R. Soc. Lond. A 2000 **358**, 2457-2470
doi: 10.1098/rsta.2000.0660

10.1098/rsta.2000.0660

Infrared absorption spectroscopy of D_3: an investigation into the formation mechanisms of triatomic hydrogenic species

By T. Amano† and Man-Chor Chan‡

Herzberg Institute of Astrophysics, National Research Council, 100 Sussex Drive, Ottawa, Ontario, Canada K1A 0R6 and Institute for Astrophysics and Planetary Sciences, Ibaraki University, 2-1-1 Bunkyo, Mito 310-8512, Japan

Infrared absorption spectra of D_3 are observed with a difference frequency laser system in the frequency ranges around 3600 cm^{-1} ($3s\,^2A_1' \leftarrow 3p\,^2E'$) and 3900 cm^{-1} ($3d \leftarrow 3p\,^2E'$). The observed line shapes exhibit a non-Maxwellian velocity distribution, and the translational energy is derived to be *ca.* 0.4 eV. From this finding, it is concluded that D_3 is formed through the dissociative recombination reaction of D_5^+ with electrons. The rotational dependence of the line shapes of the 3600 cm^{-1} band is brought about by a competition between the predissociation in the $3s\,^2A_1'$ state and the radiative decay in the $3p\,^2E'$ state. The shorter lifetimes of the 3d complex make the line shape of the 3900 cm^{-1} band simpler, a superposition of two absorption profiles with different widths. The greater widths of the absorption lines of the 3900 cm^{-1} band are attributed to unresolved spin-splittings.

Keywords: hydrogen species; infrared spectra; Rydberg state; dissociative recombination

1. Introduction

The triatomic hydrogenic radicals H_3 and D_3 have been the subject of a number of studies over the years. Rotationally resolved transitions between Rydberg states were first observed by Herzberg in emission from a hollow cathode discharge of H_2 (Herzberg 1979). Following this remarkable observation, Herzberg and co-workers carried out an extensive spectroscopic study on H_3 and D_3 to observe and analyse several emission bands between various Rydberg states (Dabrowski & Herzberg 1980; Herzberg & Watson 1980; Herzberg *et al.* 1981, 1982). Fast-neutral-beam photoionization spectra of H_3 were observed by Helm (1986), and high-n Rydberg states were identified. Cosby & Helm (1988) and Helm (1988) further measured the ionization potential and investigated the photodissociation processes. Figger and co-workers (Figger *et al.* 1989; Ketterle *et al.* 1989) also observed the emission spectra by neutralizing the parent H_3^+ ion, albeit with low resolution, and obtained the lifetimes of the Rydberg states. Bjerre *et al.* (1991) performed high-resolution laser spectroscopy of a fast neutral beam of H_3 and observed the spin-splittings in the 3d states.

† Present address: Institute for Astrophysics and Planetary Sciences, Ibaraki University, Mito, Japan.
‡ Present address: Department of Chemistry, The Chinese University of Hong Kong, Shatin, NT, Hong Kong.

The ground electronic state ($2p\,^2E'$) is repulsive. On the other hand, the excited electronic states, which can be understood as a Rydberg electron attached to an H_3^+ ion core, are bound with lifetimes ranging from a few ns to *ca.* 100 μs. The lowest bound state $2s\,^2A_1'$, which has a lifetime of *ca.* 10^{-12} s, predissociates to the repulsive ground state $2p\,^2E'$ via vibronic coupling. Several *ab initio* calculations have been performed to obtain the excitation energies and the transition dipole moments (King & Morokuma 1979; Jungen 1979; Martin 1979; Petsalakis *et al.* 1988; Peng *et al.* 1990).

Since the ground state of H_3 (and D_3) is repulsive, the Rydberg states of H_3 can only be products of chemical processes, not electronic excitation from the ground state. In the series of work conducted by Herzberg and co-workers it was suggested from circumstantial evidence, such as the fact that the cathode glow was the more favourable source of H_3 or D_3 and the enhancement of the signal at liquid nitrogen temperature, that the dissociative recombination of H_3^+ with electrons was the most likely channel to produce H_3. It was speculated at that time that the process probably involved the capture of an electron by H_3^+ to form H_3 in the Rydberg states, and the subsequent cascading through Rydberg states resulted in the emission spectra. The importance of the larger hydrogen cluster ions in the formation of H_3, however, was proposed by Miderski & Gellene (1988). By monitoring the $3s\,^2A_1' \rightarrow 2p^2A_2''$ emission band of H_3, the effect of temperature and hydrogen density on the efficiency of the production in the hollow cathode discharge was studied and the primary process leading to H_3 was interpreted to be the dissociative recombination of H_5^+ and electrons.

However, as clear-cut evidence has yet to be provided to identify the nature of the formation process of H_3, the high-resolution absorption spectroscopy of H_3 and D_3 is set out in the hope of shedding some light from linewidth and line-shape studies of the transitions. Although our attempts to observe the H_3 absorption spectra were unsuccessful, the electronic transitions of D_3 in the 3600 cm^{-1} ($3s\,^2A_1' \leftarrow 3p\,^2E'$) and in the 3900 cm^{-1} ($3d \leftarrow 3p\,^2E'$) regions do exhibit broad non-Gaussian line shapes, which provide crucial information on the formation mechanisms of the species.

2. Experiment

(*a*) *Observations*

The absorption spectra of D_3 were observed with a difference frequency laser spectrometer. The instruments used in this study have been described elsewhere and the details are not repeated here. The D_3 radical was generated by 10 kHz AC discharges of D_2 gas at pressures in the range of *ca.* 400 mTorr to 1 Torr in a hollow-cathode discharge cooled with either methanol at 213 K circulated through a refrigerated bath circulator or liquid N_2 at 77 K. It was found that the coolant temperature has little effect on the spectra and most of the spectra presented here were recorded using methanol cooling. A typical discharge current of *ca.* 600 mA was used. The absorption signals were detected using an InSb detector at 77 K and demodulated at the discharge frequency using a lock-in amplifier. It should be noted here that the line shapes obtained after the lock-in detection are 'zero-derivative' shapes, not first or second derivatives.

To aid our discussion of the D_3 spectra, figure 1 shows the low-lying Rydberg electronic states with the corresponding lifetimes. The lifetimes were calculated using

PHILOSOPHICAL TRANSACTIONS OF THE ROYAL SOCIETY A MATHEMATICAL, PHYSICAL & ENGINEERING SCIENCES

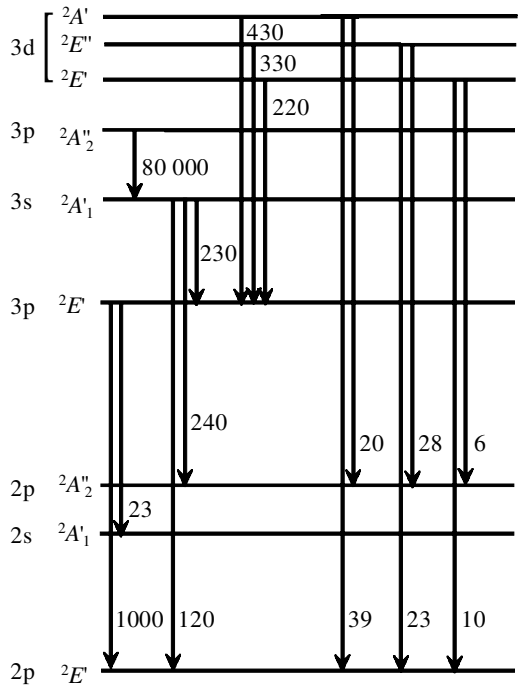

Figure 1. Schematic energy level diagram with radiative transition lifetimes calculated using *ab initio* transition dipole moments.

ab initio transition moments obtained by King & Morokuma (1979) and Petsalakis *et al.* (1988). These calculations were for the deuterated species, and the radiative lifetimes for H_3 are similar. However, predissociations occur much more readily in H_3, leading to much greater linewidths. It is interesting to note that the upper state involved in the 3600 cm^{-1} band has a longer lifetime compared with the lower state.

Two electronic bands, $3s\,^2A'_1 \leftarrow 3p\,^2E'$ and $3d \leftarrow 3p\,^2E'$, of H_3 and D_3 were studied. In the case of D_3, both bands were observed, but with different line shapes, which remain unchanged at various discharge conditions. In the case of H_3, however, neither band was observed in a variety of discharge conditions. Our unsuccessful observation of H_3 may be ascribed to the very short lifetime of this species compared with that of D_3.

Since the transitions studied involved two electronic excited states of lifetimes less than several hundreds of ns, the absorption spectra were, therefore, expected to be very difficult to observe, even though the corresponding emission spectra were found to be reasonably strong. The spectra reported by Dabrowski & Herzberg (1980) and Herzberg *et al.* (1980, 1981, 1982) revealed that transitions of D_3 exhibit sharper linewidths than those of H_3, suggesting longer lifetimes for D_3, and, therefore, more feasible for absorption spectroscopy. This was verified by our observations, as mentioned above.

The initial search was guided by the emission observations of Herzberg *et al.* (1981), and the absorption lines were readily detected. However, the line shapes were found to manifest non-thermal velocity distributions. Moreover, the line shapes vary drastically depending on the rotational states. One example is shown in figure 2

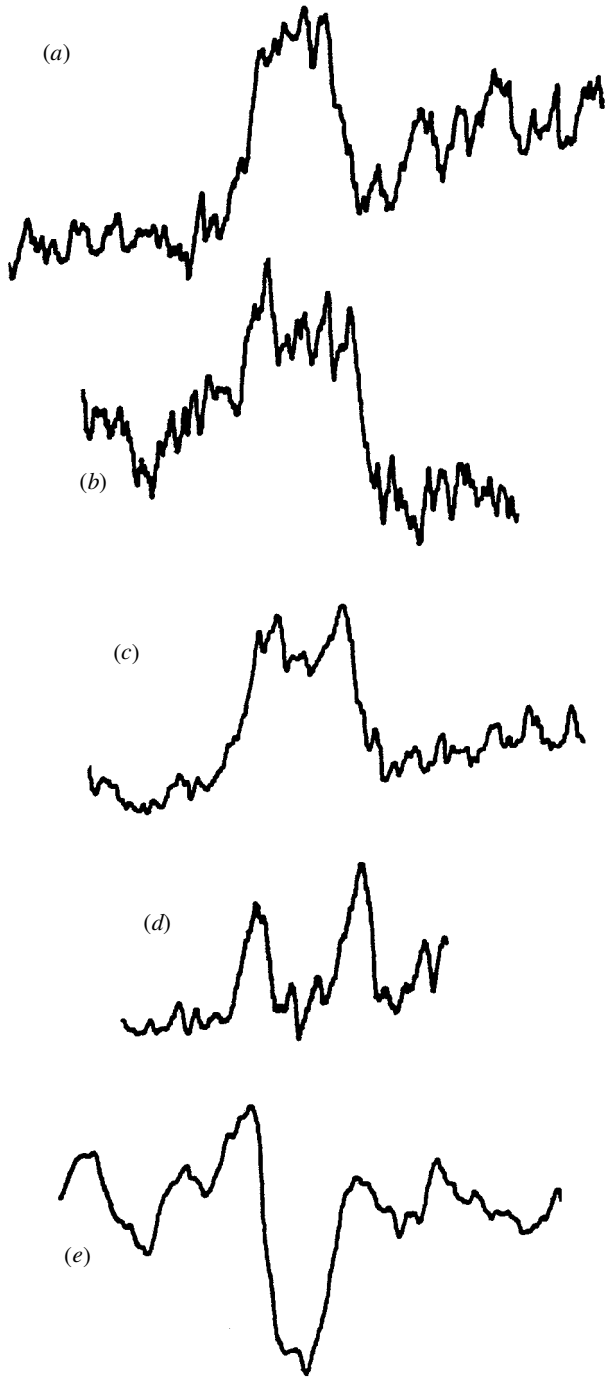

Figure 2. Examples of the absorption signals for a series of P-branch transitions, ${}^{p}P_2(N)$: (*a*) ${}^{p}P_2(6)$, (*b*) ${}^{p}P_2(5)$, (*c*) ${}^{p}P_2(4)$, (*d*) ${}^{p}P_2(3)$, (*e*) ${}^{p}P_2(2)$.

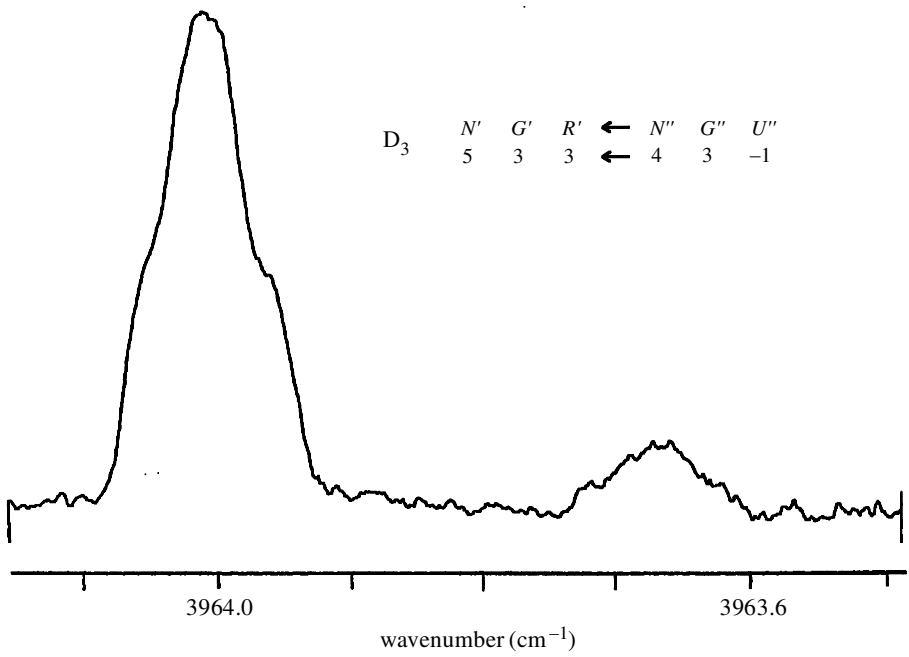

Figure 3. An example of the absorption signal of the 3900 cm^{-1} band.

for a series of lines of the $^pP_2(N)$ branch of the 3600 cm^{-1} band ($3s\,^2A_1' \leftarrow 3p\,^2E'$). These lines appear to be a superposition of two components, a broader feature and a narrower feature, for some transitions with the opposite phase. The observed line profiles can be rationalized by a superposition of an absorption line and an emission line. The phase conventions will be described in the next section. The widths of the two constituents vary depending on the translational energies in the lower and upper states. The resultant shape of the transition, therefore, depends on the relative intensities and the widths of both constituents.

The lines of the 3900 cm^{-1} band ($3d \leftarrow 3p\,^2E'$) also exhibit a non-trivial shape. However, unlike the 3600 cm^{-1} band, two components with different widths are superposed with the same phase, as illustrated in figure 3, and the line profile does not depend appreciably on the rotational state. Although the collisional cross-sections for these transitions are not known, the line shapes indicate that the distribution is non-thermal and retains the nascent velocity distribution without collisional disturbance. Thus, the investigation of these line shapes is of prime interest for our discussions.

(*b*) *Phase optimization*

Since the line shapes of the absorption lines were neither Gaussian nor Voigt shapes, and they varied depending on the transitions, we examined whether the shape depended on the phase setting of the lock-in amplifier. In the same region of the 3600 cm^{-1} band, we also observed the $2\nu_2$ overtone band of D_3^+. We therefore used the optimum phase of D_3^+ signals as a guide to obtain the optimum phase of D_3. It was found that the optimum phase of D_3 was *ca.* 30° delayed from that of

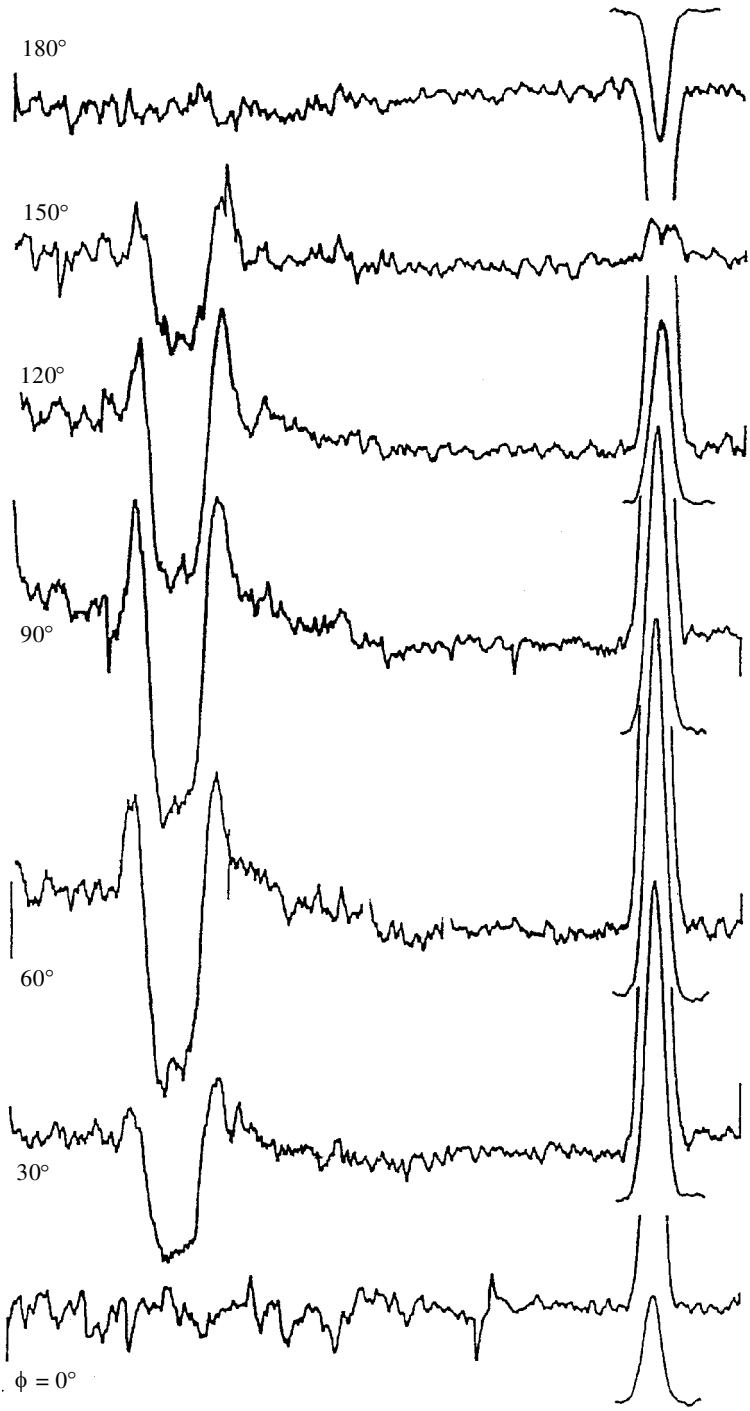

Figure 4. Lock-in phase dependence of the intensity of a D_3 line of the 3600 cm^{-1} band relative to a line of $2\nu_2$ band of D_3^+.

PHILOSOPHICAL TRANSACTIONS OF THE ROYAL SOCIETY A MATHEMATICAL, PHYSICAL & ENGINEERING SCIENCES

D_3^+. This phase delay corresponded to a time delay of *ca.* 8 μs. Figure 4 shows the effect of the phase settings on the $^pP_4(4)$ line of the $3s\,^2A_1' \leftarrow 3p\,^2E'$ band of D_3, which is in the vicinity of a D_3^+ line. It is seen that the phase settings only changed the observed intensity of the transition but had little effect on the line shape. The spectra reported here were, therefore, measured at the optimum phase. Throughout this paper, line profiles pointing upwards mean absorption.

(*c*) *Observed line shape and linewidth*

The emission lines observed by Herzberg *et al.* (1981) also showed a broad linewidth, which was attributed to the Doppler width corresponding to the kinetic temperature of 3000 K, although the shape appeared to be normal, presumably due to the low spectral resolution employed in their Fourier-transform spectrometer, 0.12 cm^{-1}.

Figure 5 shows the $^pP_4(4)$ and $^pQ_1(2)$ transitions of the 3600 cm^{-1} ($3s\,^2A_1' \leftarrow 3p\,^2E'$) band exhibiting very different shapes: while the $^pQ_1(2)$ line is an 'absorption' line, the $^pP_4(4)$ transition appears to be an 'emission' line.

In addition to the shape variation discussed above, all observed lines exhibit flat-top shapes in the high-resolution spectra, as expected from species with a non-Maxwellian distribution of kinetic (translational) energy. The appearance of these line shapes immediately suggests that the species is produced from a higher member of hydrogenic clusters. It is almost impossible to form such species with high translational energy from the dissociative recombination of $D_3^+ + e^-$. Rogers & Biondi (1964) derived the line-shape function for the case of two equal-mass fragments produced from the disintegration of a larger parent energetic species. Miderski & Gellene (1988) extended the formulation to a case of unequal mass fragments. Here we reproduce their result for convenience for the discussions to follow,

$$G(\nu) = (a/4b)[\mathrm{erf}(a\nu + b) - \mathrm{erf}(a\nu - b)], \tag{2.1}$$

where ν is the transition wavenumber relative to the line centre and erf represents the error function. In this equation, a and b are defined thus:

$$a = \left(\frac{Mc^2}{2kT_g}\right)^{1/2} \Big/ \nu_0 \quad \text{and} \quad b = \left(\frac{m_2 E_D}{m_1 k T_g}\right)^{1/2},$$

with the following definitions: ν_0 is the wavenumber of the line centre, M is the total mass $(m_1 + m_2)$, and m_1 is the mass of the observed fragment. The gas kinetic temperature is designated as T_g and the total kinetic energy release is expressed as E_D. When the total kinetic energy shared by the two fragment molecules is much larger than the gas kinetic energy, $b \gg 1$, and the linewidth is given by

$$\Delta\nu = \frac{b}{a} = \left(\frac{2m_2 E_D}{m_1 M}\right)^{1/2} \frac{\nu_0}{c}. \tag{2.2}$$

The line-shape function given by equation (2.1) reproduces the observed one given in figure 5*a* except for a slight sag at the central part, by assuming D_3 generated from D_5^* and the total kinetic energy release being 1 eV. By considering the partition of the translational energy between D_3 and D_2, the kinetic energy of D_3 was derived to be *ca.* 0.4 eV.

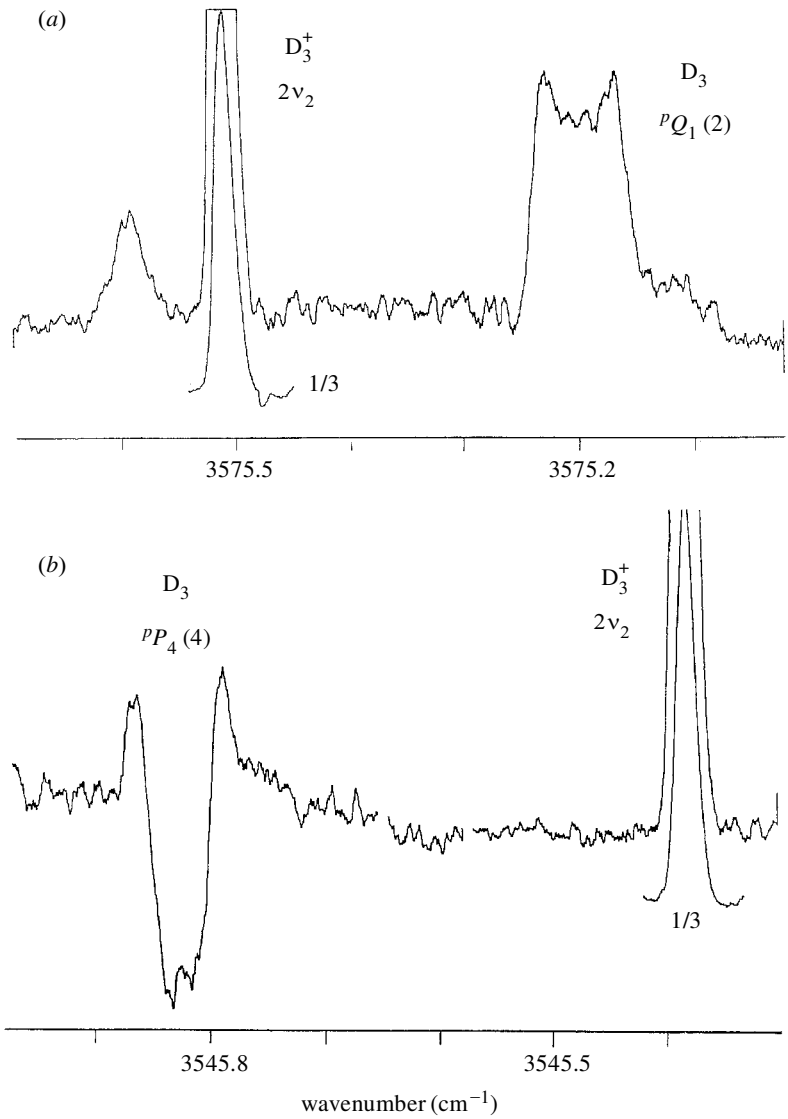

Figure 5. Examples of two distinct line shapes observed for the 3600 cm^{-1} band. (*a*) $^pQ_1(2)$ transition, (*b*) $^pP_4(4)$ transition.

3. Discussion

The half-width at half-maximum (HWHM) was measured to be 0.043 cm^{-1} for the $^pQ_1(2)$ transition (see figure 5*a*), and it corresponds to a kinetic energy of 0.4 eV or a translational temperature of 4600 K, as described above. Miderski & Gellene (1988) assumed that H_3 is produced through the dissociative recombination of H_5^+, and obtained the total kinetic energy release (i.e. kinetic energy carried away by H_3 *and* H_2) of 0.7 ± 0.1 eV. The kinetic energy release determined by Miderski & Gellene (1988) and by this work seems to support the idea that H_3 or D_3 neutrals are produced through the dissociative recombination of H_5^+ or D_5^+.

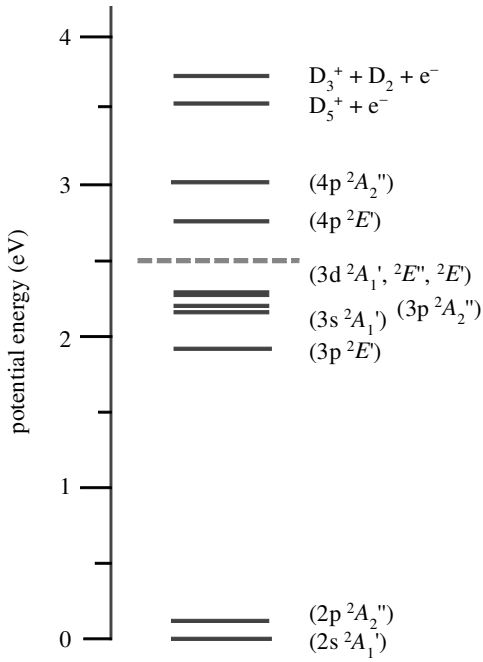

Figure 6. Relative energies for D_3^*, $D_3^+ + e^-$, and $D_5^+ + e^-$.

Figure 6 indicates the relative energies of the neutral species, D_3^+ and the $D_5^+ + e^-$ limit, similar to fig. 6 of Miderski & Gellene (1988). The dashed line indicates 1 eV below the energy of $D_5^+ + e^-$. It is located below the $n = 4$ levels. The kinetic energy release upon the dissociation of D_5^+ is consistent with, and confirms, the non-observation of the emission from $n = 4$ and higher electronic states.

The next question is how the line shapes and their rotational dependence are to be understood. We assume that D_3 is supplied to each state through two distinct paths: a direct supply from the dissociative recombination of D_5^+ and a cascade from the upper states. The molecules cascaded down from the upper states have less kinetic energy, resulting in smaller Doppler widths. Although, in the emission spectra of the 3600 cm^{-1} band of Herzberg *et al.* (1981), no substantial predissociation was evident with their spectral resolution, our observation of the N, K-dependence of the line shape can be caused by the inhomogeneous predissociations in the $3s\,^2A_1'$ state, the upper state of the infrared transition. The predissociation probability is proportional to

$$N(N+1) - K^2. \tag{3.1}$$

The line shapes of the 3900 cm^{-1} band, which shares the common lower state with the 3600 cm^{-1} band, are quite different, as demonstrated in figure 3 with no substantial rotational state dependence. This fact is further support for the assumption that the predissociations are in the upper state not in the lower state.

The absorption coefficient, γ, is given by

$$\gamma = (N_1 - N_2)\sigma, \tag{3.2}$$

where N_1 and N_2 are the populations of the lower and upper states, respectively, and σ is the absorption cross-section. We assume that there are two components for N_1. One is a direct supply from the dissociative recombination of D_5^+. The other is a cascaded population from the upper states, in particular from the $3s\,^2A_1'$ state, judging from the calculated radiative lifetimes for the individual transitions. On the other hand, the supply of N_2 is basically only the direct process. Therefore, the populations, N_1 and N_2, are written more specifically as

$$N_1(v) = N_1^{\mathrm{dir}}(v) + N_1^{\mathrm{cas}}(v), \tag{3.3}$$

$$N_2(v) = N_2^{\mathrm{dir}}(v). \tag{3.4}$$

Because N_1^{cas} is cascaded from N_2^{dir}, the velocity distribution for these two is the same. Then the absorption coefficient is rewritten as

$$\gamma = [\bar{N}_1^{\mathrm{dir}} V(v_1) - (\bar{N}_2^{\mathrm{dir}} - \bar{N}_1^{\mathrm{cas}}) V(v_2)]\sigma, \tag{3.5}$$

where $V(v_1)$ and $V(v_2)$ are the velocity distribution functions for N_1^{dir} and N_2^{dir}, respectively, and $V(v_1)$ has a broader distribution than $V(v_2)$. The populations designated with an overbar, $\bar{N}_1^{\mathrm{dir}}$, etc., mean the integrated population over the entire velocity distribution. The observations presented in this investigation indicate that the population difference, $\bar{N}_2^{\mathrm{dir}} - \bar{N}_1^{\mathrm{cas}}$, is a function of $N(N+1) - K^2$, suggesting that the inhomogeneous predissociations in the upper state of the transition play an important role. For the $N \simeq K$ transitions, $\bar{N}_2^{\mathrm{dir}} > \bar{N}_1^{\mathrm{cas}}$, while $\bar{N}_2^{\mathrm{dir}} \simeq \bar{N}_1^{\mathrm{cas}}$ for the transitions with $N \gg K$, as a result of the competition between the predissociation in the upper state and the radiative decay in the lower state.

A similar discussion can be applied to the interpretation of the line shapes of the 3900 cm^{-1} band. Unlike the 3600 cm^{-1} band, however, the line shape appears as the line shape shown in figure 3 for all the observed transitions. Since the lower state is common to the 3600 cm^{-1} and 3900 cm^{-1} bands, it is surprising to see such different appearances in the line shapes for the 3900 cm^{-1} band compared with those in the 3600 cm^{-1} band. Because the lifetimes of the 3d complex are much shorter than those of the $3p\,^2E'$ state, $\bar{N}_1^{\mathrm{cas}}$ turned out to be larger than $\bar{N}_2^{\mathrm{dir}}$ for all the transitions from the 3900 cm^{-1} band, resulting in superpositions of two absorption features with different widths.

The width of the broader component of the transitions of the 3900 cm^{-1} band ($3d \leftarrow 3p\,^2E'$) is found to be 0.063 cm^{-1} (HWHM). The corresponding width for the 3600 cm^{-1} band ($3s\,^2A_1' \leftarrow 3p\,^2E'$) is 0.043 cm^{-1}, and this translates to 0.048 cm^{-1} for the 3900 cm^{-1} band after correcting for the difference of the transition wavenumbers. So the observed width is larger by 0.018 cm^{-1} than that in the 3600 cm^{-1} band. As these bands share the common lower state, $3p\,^2E'$, it is certainly puzzling to have such a discrepancy in the widths. The 3d complex exhibits heavy mixing among the three states due to the electronic Coriolis interaction. The 3900 cm^{-1} transition carries basically the characteristics of an E–E type transition. Bjerre *et al.* (1991) measured the spin-doublings of several rotational levels of the 3d states by using fast-neutral-beam laser spectroscopy. The spin-orbit coupling constant derived was *ca.* 430 MHz. The splittings are dependent on the rotational quantum numbers, but the extra broadening we observed is consistent with the magnitude of the spin-doubling.

Now, is the abundance of D_3 obtained in this experiment reasonable, if the dominant channel is the dissociative recombination of D_5^+? Figure 7 illustrates a simplified

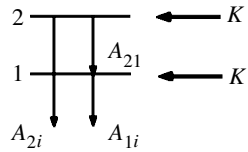

Figure 7. Schematic to show formation and decay processes.

energy-level scheme to calculate the steady-state abundance of D_3. In this model, D_3 is supplied by the dissociative recombination reaction of D_5^+ with electrons with the rate K s^{-1} equally for the upper and the lower states, and A_{ij} are the radiative transition rate coefficients, which can be calculated by using the *ab initio* transition moments. We obtain a set of rate equations:

$$\frac{\mathrm{d}N_1}{\mathrm{d}t} = K + A_{21}N_2 - A_{1i}N_1, \tag{3.6}$$

$$\frac{\mathrm{d}N_2}{\mathrm{d}t} = K - (A_{21} + A_{2i})N_2. \tag{3.7}$$

In the equations above, A_{1i} and A_{2i} are defined as the sum of the A coefficients of all other possible transitions from states 1 and 2, respectively. At the steady state,

$$N_2 = \frac{K}{A_{21} + A_{2i}}, \tag{3.8}$$

$$N_1 = \frac{K}{A_{1i}}\left(1 + \frac{A_{21}}{A_{21} + A_{2i}}\right), \tag{3.9}$$

and

$$N_1 - N_2 = \frac{2A_{21} + A_{2i} - A_{1i}}{A_{1i}(A_{21} + A_{2i})}K. \tag{3.10}$$

The abundance was estimated to be $N_1 \sim 3 \times 10^4$ cm^{-3} from the $^pQ_1(2)$ line intensity by assuming the *ab initio* transition dipole moment, and this value leads to $K = 1.2 \times 10^{12}$ cm^{-3} s^{-1}. This abundance is for this particular quantum state. We do not have detailed information on the rotational population distribution. For a rough estimate, we assume the total formation rate of D_3 to be approximately two orders of magnitude larger: $K_t \sim 100K = 1.2 \times 10^{14}$ cm^{-3} s^{-1}. The rate K_t should be given by

$$K_t = \alpha[\mathrm{H}_5^+][\mathrm{e}^-], \tag{3.11}$$

and if

$$\alpha \sim 2 \times 10^{-6}\ \mathrm{cm}^3\ \mathrm{s}^{-1}, \tag{3.12}$$

$$[\mathrm{e}^-] \sim 10^{11}\ \mathrm{cm}^{-3} \tag{3.13}$$

are assumed, we obtain $[\mathrm{H}_5^+] \sim 6 \times 10^8$ cm^{-3}.

On the other hand, H_5^+ should be formed by

$$\mathrm{H}_3^+ + 2\mathrm{H}_2 \rightarrow \mathrm{H}_5^+ + \mathrm{H}_2, \tag{3.14}$$

$$\mathrm{H}_5^+ + \mathrm{e}^- \rightarrow \mathrm{H}_3 + \mathrm{H}_2, \tag{3.15}$$

and, at the steady state, the abundance of H_5^+ is given by

$$[H_5^+] = \frac{k}{\alpha}\frac{[H_3^+][H_2]^2}{[e^-]}, \tag{3.16}$$

where k and α are the rate coefficients for the formation of H_5^+ and the dissociative recombination, respectively. The rate coefficient k was obtained by Hiraoka & Kebarle (1975) to be $k = 9 \times 10^{-30}\ \mathrm{cm^6\ s^{-1}}$. By using the known abundance of H_2 (*ca.* $6 \times 10^{15}\ \mathrm{cm^{-3}}$) and by assuming $[H_3^+] \sim [e^-]$, we obtain $[H_5^+] \sim 2 \times 10^8\ \mathrm{cm^{-3}}$, the same order of magnitude as the value obtained from the intensity measurements.

4. Conclusion

Two infrared Rydberg bands of D_3—the 3600 $\mathrm{cm^{-1}}$ ($3s\,^2A_1' \leftarrow 3p\,^2E'$) and the 3900 $\mathrm{cm^{-1}}$ ($3d \leftarrow 3p\,^2E'$) bands—have been observed in absorption. The observation of the corresponding bands for H_3 has been unsuccessful. The line shapes are neither Doppler nor Lorentzian. Rather, they consist basically of two flat-topped components with different widths. In the 3600 $\mathrm{cm^{-1}}$ band, a quite conspicuous rotational dependence of the shape was exhibited: some transitions showed the narrower component superposed with the opposite phase, resulting in an emission feature. The rotational dependence is very probably a result of the competition between the predissociation in the upper state, $3s\,^2A_1'$, and the radiative decay process in the lower state, $3p^2E'$. The widths correspond to the translational energy of *ca.* 0.4 eV. From this observation, it was concluded that D_3 was formed through the dissociative recombination of D_5^+. The origin of two components was interpreted to be (1) direct formation channel, and (2) cascading processes from upper states.

The line shape of the 3900 $\mathrm{cm^{-1}}$ band appears to be a superposition of two components similar to those observed in the 3600 $\mathrm{cm^{-1}}$ band. However, it exhibits no noticeable rotational dependence, unlike the 3600 $\mathrm{cm^{-1}}$ band: superposition of the two components with the same absorption feature. This was understood as the result of shorter lifetimes of the 3d states compared with the lower state of the transition, $3p\,^2E'$. The velocity distribution derived from the width of the lines of the 3900 $\mathrm{cm^{-1}}$ band was found to be wider compared with that derived from the 3600 $\mathrm{cm^{-1}}$ band lines. This discrepancy was probably due to unresolved spin splittings of the transitions of the 3900 $\mathrm{cm^{-1}}$ band.

Several points are worth further investigation in the future. One is the temperature dependence. In the series of experiments by Herzberg and co-workers, it was described that the cooling of the hollow-cathode discharge cell to liquid nitrogen temperature was essential to obtain the emission spectra. Our observation indicates a much smaller temperature dependence of the absorption intensity. As described already in this paper, our spectra were mostly recorded at 213 K. We found that no substantial increase of the absorption intensity was achieved at liquid nitrogen temperature. If the formation process is the dissociative recombination of D_5^+, a much more conspicuous temperature dependence is likely to show up. Second, the greater linewidths of the 3900 $\mathrm{cm^{-1}}$ band are ascribed to the unresolved spin-doublings. To verify this, more systematic and extensive rotational dependence of the widths should be investigated. The third point we would like to make is that many more

unassigned lines, which are clearly due to D_3 absorption judged from the broad feature, are observed. More spectroscopic investigation is worth pursuing, in particular for the 3900 cm^{-1} band.

We thank J. K. G. Watson for elucidating discussion. Very recently some of the measurements were repeated at Professor Momose's laboratory at Kyoto University. T.A. thanks T. Momose, his graduate students, M. Fushitani and H. Katsuki, and two graduate students from Ibaraki University, M. Yamada and Y. Yoshida, for their help in the measurements. This work was supported in part by grants from the Ministry of Education, Science, and Culture of Japan (nos 060037429, 08044054 and 9044056).

References

Bjerre, N., Hazell, I. & Lorents, D. C. 1991 *Chem. Phys. Lett.* **181**, 301–306.
Cosby, P. C. & Helm, H. 1988 *Phys. Rev. Lett.* **61**, 298–301.
Dabrowski, I. & Herzberg, G. 1980 *Can. J. Phys.* **58**, 1238–1249.
Figger, H., Ketterle, W. & Walther, H. 1989 *Z. Phys.* D*: Atoms, Molecules Clusters* **13**, 129–137.
Helm, H. 1986 *Phys. Rev. Lett.* **56**, 42–45.
Helm, H. 1988 *Phys. Rev.* A **38**, 3425–3429.
Herzberg, G. 1979 *J. Chem. Phys.* **70**, 4806–4807.
Herzberg, G. & Watson, J. K. G. 1980 *Can. J. Phys.* **58**, 1250–1258.
Herzberg, G., Lew, H., Sloan, J. J. & Watson, J. K. G. 1981 *Can. J. Phys.* **59**, 428–440.
Herzberg, G., Hougen, J. T. & Watson, J. K. G. 1982 *Can. J. Phys.* **60**, 1261–1284.
Hiraoka, K. & Kebarle, P. 1975 *J. Chem. Phys.* **63**, 746–749.
Jungen, M. 1979 *J. Chem. Phys.* **71**, 3540–3541.
Ketterle, W., Figger, H. & Walther, H. 1989 *Z. Phys.* D*: Atoms, Molecules Clusters* **13**, 139–146.
King, H. F. & Morokuma, K. 1979 *J. Chem. Phys.* **71**, 3213–3220.
Martin, R. L. 1979 *J. Chem. Phys.* **71**, 3541–3542.
Miderski, C. A. & Gellene, G. I. 1988 *J. Chem. Phys.* **88**, 5331–5337.
Peng, Z., Kuppermann, A. & Wright, J. S. 1990 *Chem. Phys. Lett.* **175**, 242–248.
Petsalakis, I. D., Theodorakopoulos, G. & Wright, J. S. 1988 *J. Chem. Phys.* **89**, 6850–6859.
Rogers, W. A. & Biondi, M. A. 1964 *Phys. Rev.* A **134**, 1215–1225.

Discussion

J. B. A. Mitchell (*PALMS, Université de Rennes, France*). About ten years ago, Herzberg tried without success to see the spectrum of D_2H. Has this been achieved?

T. Amano. Two mixed isotopic species of H_3, H_2D and HD_2, were observed and the results have been published in a monograph dedicated to C. H. Townes on his 80th birthday (Dabrowski & Herzberg 1996).

G. Duxbury (*Department of Physics and Applied Physics, University of Strathclyde, UK*). In his paper Professor Amano has commented upon the complex absorption line shapes which he has observed, and which he has indicated are caused by the competition between the two methods of populating each of the energy levels between which the inter-Rydberg state transitions occur. These two processes are the direct method of populating a particular level via formation in a given state via dissociative recombination of H_5^+, and cascading from higher populated levels. Two types of absorption line shape in the concentration modulation spectra have been shown in his presentation, the 'hole' in inter-Rydberg state transitions in the 3600 cm^{-1}

band, and the 'spike' in absorption lines of the 3900 cm^{-1} band. I would be grateful if he could give further details on the rates of the competing processes in the two bands in order to explain further the occurrence of the 'holes' and 'spikes'. Since the pedestals which are attributed to direct formation, and which are associated with a measurement of kinetic energy release, appear to have different widths in the two bands, could Professor Amano expand a little his explanation of the differences in the kinetic energy release for these two-band systems.

T. Amano. Whether the second component becomes a 'spike' or a 'hole' depends on the sign of the second term of equation (3.5). For the 3600 cm^{-1} band, the magnitude of the second term varies depending on the rotational quantum numbers. The reason for the occurrence of the rotational dependence is, as explained in the text, a competition between the predissociations and the radiative decay in the upper state of the transition. If equations (3.6) and (3.7) are modified to include the predissociations, we obtain

$$N_2^{\mathrm{dir}} - N_1^{\mathrm{cas}} = \frac{K}{A_{21} + A_{2i} + P}\left(1 - \frac{A_{21}}{A_{1i}}\right). \tag{4.1}$$

We estimate $A_{21}/A_{1i} \sim 1/10$ by assuming the calculated radiative lifetimes. The predissociation rate P is given by

$$P = D[N(N+1) - K^2]. \tag{4.2}$$

Therefore, for the states with $N \gg K$,

$$N_2^{\mathrm{dir}} - N_1^{\mathrm{cas}} \simeq \frac{K}{A_{21} + A_{2i} + P} < \frac{K}{A_{1i}} = N_1^{\mathrm{dir}}, \tag{4.3}$$

if P is comparative with or larger than A_{1i}. Here, the line shape appears as a pedestal. On the other hand, for the states with $N \sim K$, P can be negligible compared with $A_{21} + A_{2i}$. As a result,

$$N_2^{\mathrm{dir}} - N_1^{\mathrm{cas}} \simeq \frac{K}{A_{21} + A_{2i}} > \frac{K}{A_{1i}} = N_1^{\mathrm{dir}}, \tag{4.4}$$

causing a 'hole'. However, the predissociation in the upper state discussed here is not a great effect to be detected by the low-resolution infrared emission experiment of Herzberg *et al.* (1981).

The lifetime of the upper state of the 3900 cm^{-1} band, 3d complex, is of the order of 10 ns, which is much shorter than the lifetime of the lower state, $3p\,^2E'$. Therefore, no matter what the rotational state is, $N_2^{\mathrm{dir}} < N_1^{\mathrm{cas}}$, resulting in a superposition of 'spikes'.

At first glance, the greater linewidths of the transitions of the 3900 cm^{-1} band are puzzling. The extra broadening of the lines of the 3900 cm^{-1} band is likely to be the larger spin-orbit splitting in the upper states, 3d complex. Bjerre *et al.* (1991) determined the spin-orbit coupling constant to be *ca.* 430 MHz, which is consistent with the amount of the extra broadening we observed. However, more quantitative investigation, such as the rotational dependence of the widths, should be pursued.

Additional reference

Dabrowski, I. & Herzberg, G. 1996 The electronic emission spectra of triatomic hydrogen: the 6025 Å bands of H_2D and HD_2. In *Amazing light* (ed. R. Y. Chiao), pp. 173–190. Springer.